

# On the freshwater forcing and transport of the Atlantic thermohaline circulation

S. Rahmstorf\*

Institut für Meereskunde, D-24105 Kiel, Germany

Received: 10 February 1996 / Accepted: 30 May 1996

**Abstract.** The ‘conveyor belt’ circulation of the Atlantic Ocean transports large amounts of heat northward, acting as a heating system for the northern North Atlantic region. It is widely thought that this circulation is driven by atmospheric freshwater export from the Atlantic catchment region, and that it transports freshwater northward to balance the loss to the atmosphere. Using results from a simple conceptual model and a global circulation model, it is argued here that the freshwater loss to the atmosphere arises mainly in the subtropical South Atlantic and is balanced by northward freshwater transport in the wind-driven subtropical gyre, while the thermohaline circulation transports freshwater southward. It is further argued that the direction of freshwater transport is closely linked to the dynamical regime and stability of the ‘conveyor belt’: if its freshwater transport is indeed southward, then its flow is purely thermally driven and inhibited by the freshwater forcing. In this case the circulation is not far from Stommel’s saddle-node bifurcation, and a circulation state without NADW formation would also be stable.

## 1 Introduction

The Atlantic is the only ocean which produces deep water in the Northern Hemisphere. North Atlantic Deep Water (NADW) is formed by convection in the Norwegian and Labrador Seas, and moves south at a depth of 2–3 km until it joins the Antarctic Circumpolar Current (Warren 1981). Compensating the southward flow is a warmer, shallower northward flow. This overturning circulation, with a volume transport of about 17 Sv (Roemmich and Wunsch 1985; 1 Sverdrup =  $10^6$  m<sup>3</sup>/s), leads to the ‘anomalous’ heat transport of the Atlantic: unlike the Pacific and Indian

oceans, which move heat from the tropics to the high-latitudes of both hemispheres, the Atlantic transports heat northward at all latitudes, even south of the equator. As a consequence, the northern North Atlantic is about 4°C warmer than comparable latitudes in the Pacific (Levitus 1982). The NADW circulation thus has a strong effect on regional climate, and mounting palaeoclimatic evidence links past temperature shifts to changes in NADW flow (Broecker et al. 1985; Boyle and Keigwin 1987; Keigwin et al. 1994; Sarin et al. 1994).

The formation of NADW and the associated deep overturning cell (see Fig. 9) are part of the global thermohaline circulation, which is driven by density differences. These density differences are ultimately generated by heat and freshwater fluxes at the ocean surface. The purpose of this study is to clarify the role of freshwater fluxes in forcing the flow of NADW, since different views about this role prevail in the oceanographic literature: on one hand freshwater forcing is seen to *drive* NADW flow, on the other hand it is seen to *brake* the flow.

The atmospheric freshwater transport from low- to high-latitudes in the Atlantic, and the corresponding net precipitation in the formation region of NADW, are usually seen as braking the flow of the ‘conveyor belt’. This idea is very clearly demonstrated in Stommel’s (1961) classical box model. In this conceptual model of thermohaline flow, one box represents low-latitudes, the second box high-latitudes, and the overturning flow is proportional to the density difference between the boxes. With atmospheric vapour transport from low- to high-latitudes, this model has two stable equilibria: a thermally driven flow with deep water forming in the cold high-latitudes, and a haline driven flow with deep water forming in the saline tropics. The thermally driven circulation is inhibited by freshwater forcing, and for increasing vapour transport the thermal solution branch ends in a saddle-node bifurcation. Although this model considers only a thermohaline overturning cell within one hemisphere, it has been widely accepted as representing the basic mechanism

\* Present address: Potsdam Institute for Climate Impact Research (PIK), PO Box 601203, D-14412 Potsdam, Germany

governing NADW formation (e.g. Weaver and Hughes 1992; Marotzke 1994). It is generally used to explain the occurrence of two distinct equilibria, with and without NADW formation, in general circulation models (e.g., Bryan 1986).

On the other hand, a number of authors have attributed NADW formation to the high evaporation rate in the Atlantic (e.g. Weyl 1968; Reid 1979; Warren 1983; Broecker and Denton 1989; Schmitt et al. 1989; Broecker et al. 1990b; Broecker 1991; Zaucker and Broecker 1992); in particular the papers (co-)authored by W. Broecker discuss this idea in detail. In this concept the NADW flow is driven by atmospheric freshwater transport, though here this is not the transport from low- to high-latitudes, but rather the net transport out of the Atlantic catchment area north of about 30°S (where the Atlantic is bounded by continents on both east and west), estimated to be about 0.35 Sv (Broecker et al. 1990b; Zaucker and Broecker 1992).

There appears to be a 'weak' and a 'strong' form of this idea. The weak form simply states that due to the atmospheric vapour export from the Atlantic, the Atlantic is saltier and the NADW circulation is stronger than it would be in the absence of this vapour export. This is obviously true; the salinity-enhancing effect of Atlantic vapour export is seen simply as competing with the freshening due to the low-to-high latitude vapour transport, with no judgment as to what the overall effect of the two competing fluxes is.

The strong form of the concept goes further (Broecker 1991; Zaucker and Broecker 1992): it proposes that the *overall* effect of the freshwater forcing felt by the 'conveyor belt' in the Atlantic is a net freshwater loss (i.e. salinity enhancement) along its route; that this freshwater loss (taken to be equal to the atmospheric vapour export from the Atlantic catchment mentioned above) is what ultimately drives the 'conveyor belt'; and that the volume transport of NADW is directly proportional to this freshwater loss. This is a picture that clearly differs from Stommel's (1961) thermally driven flow; e.g. the flow would not undergo Stommel's saddle-node bifurcation for increased freshwater input if it is proportional to the freshwater forcing. Note that a salinity enhancement along the conveyor's route implies that the southward NADW outflow at 30°S is saltier than the northward, upper branch, so that there is a *northward* freshwater transport by the 'conveyor belt' across this latitude. This northward freshwater transport balances the evaporative freshwater loss from the basin in Broecker's concept. If the 'conveyor belt' were slowed down for some time, the northward freshwater transport would be reduced and the salinity would rise in the Atlantic, eventually causing the NADW flow to increase again and thus allowing a 'salt oscillation' which was suggested as an explanation for glacial climate cycles by Broecker et al. (1990a) and Birchfield and Broecker (1990).

Stommel (1980) and Piola and Gordon (1986) have attempted to balance the observed vapour loss north of 30°S in the Atlantic by a vertical overturning circulation consisting of a northward flow of thermocline and

intermediate waters and a southward flow of deep water. Their calculations revealed that such a balance is not possible with realistic rates of NADW flow, leading Stommel to conclude that "something is wrong".

The aim of this study is to examine the respective roles of the atmospheric freshwater transport from low- to high-latitudes and the vapour export from the Atlantic catchment in forcing the NADW circulation, and to find out what is wrong with the budget calculation originally considered by Stommel (1980). I will argue that the low-to-high-latitude vapour transport within the North Atlantic has little effect on the equilibrium volume transport of NADW (in contrast to Stommel's 1961 box model), it being controlled instead by the 'active' freshwater forcing (i.e. the net salinity change) that the conveyor belt experiences en route through the Atlantic. This 'active' freshwater forcing is not easily related to the net surface freshwater flux of the Atlantic catchment, as freshwater added further south is less effective than freshwater added further north, and the wind-driven circulation plays a major role in the freshwater budget. In fact, it is argued that the 'active' freshwater forcing of the conveyor belt is a net freshening, not a net evaporation as in Broecker's concept. Consequently, freshwater transport by the conveyor belt is *southward*, and it is purely thermally driven. This has implications for the stability of the conveyor belt in past and future climatic changes, as we will discuss in detail below.

## 2 Conceptual model of the Atlantic conveyor belt

In this section, a conceptual model of the thermohaline circulation is introduced which extends Stommel's box model to cross-hemispheric flow, making it directly applicable to NADW formation (Fig. 1). This is similar to the models discussed by Rooth (1982) and Marotzke

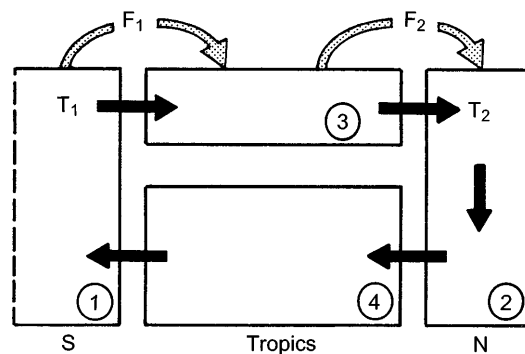


**Fig. 1.** A simple 4-box model of cross-hemispheric thermohaline flow. North Atlantic Deep Water forms in box 2; its outflow towards box 1 is controlled by the density difference between boxes 2 and 1. Salinities in the boxes are determined by the flow and the surface freshwater fluxes entering boxes 1, 2 and 3. Only two of these three fluxes are independent, since their sum must vanish in a steady state. Therefore the surface freshwater fluxes are portrayed as two atmospheric vapour transports  $F_1$  and  $F_2$ , whose significance is discussed in the text

(1990). Thual and McWilliams (1992) have analyzed the bifurcation behaviour of a hierarchy of box models. In their terminology, the present model is a 1-2-1 box model. However, a crucial difference of the present model from the ones discussed by Marotzke (1980) and Thual and McWilliams (1992) is that we allow no vertical flow between boxes 3 and 4 (i.e. across the tropical thermocline), so that the NADW circulation is modelled as a closed loop driven by density gradients between its northern and southern ends, rather than consisting of two hemispheric overturning loops, driven independently by gradients within each hemisphere. The reason for this is that in the GCM, NADW circulation appears as just such a continuous, cross-equatorial flow system (in spite of some local upwelling near 40°N, the cause of which is discussed in Böning et al. 1995). The concepts of evaporation-driven and freshwater-inhibited flow might be reconciled if the first applies to a Southern Hemisphere overturning cell and the second to a Northern Hemisphere overturning cell, which combine to a NADW flow according to the “superposition principle” of Thual and McWilliams (1992). For a continuous conveyor belt loop through the Atlantic, however, only one of the two can be true: it is either driven by evaporation or inhibited by freshwater input.

In our box model, surface temperatures can be forced by a restoring condition or, neglecting the feedback effect of the flow on temperature (Rahmstorf and Willebrand 1995), simply prescribed. Salinity forcing consists of fixed atmospheric vapour transports between the upper boxes, converted to an equivalent salt transport by multiplication with  $-S_0$ , a fixed reference salinity. This means that for the box model (and likewise for the GCM experiments discussed later), we only consider the effect of freshwater forcing on salinity, neglecting its effect on the mass balance. This approach is legitimate for our purpose; it makes freshwater transport equivalent to salt transport in the opposite direction. Using a fixed reference salinity of 35 psu in the conversion, rather than actual salinity, introduces only a negligible error. Note that the freshwater transport defined in this way does not include the throughflow from the Bering Strait. Model experiments of Reason and Power (1994) have shown that the Bering Strait flow passes through the Atlantic with little effect on salinity or deep water formation.

The flow in our box model is proportional to the density difference between the northern and southern ends of the overturning cell. The northern end is the NADW formation region, the southern end may be considered as the region south of the Cape of Good Hope, where NADW leaves the confinement between continental barriers and is blended into the circumpolar current. This is where the applicability of the box model ends. For the basic argument it is not important whether NADW rises there to close the loop, or whether it follows a more complex route governed by dynamics outside the scope of the model. We will consider equilibrium conditions; then box 4 plays no role ( $S_4 = S_2$ ) and the steady state equations are

$$m(S_2 - S_1) = -S_0 F_1 \quad (1)$$

$$m(S_3 - S_2) = S_0 F_2 \quad (2)$$

$$m = k(\rho_2 - \rho_1) = k[\beta(S_2 - S_1) - \alpha(T_2 - T_1)] \quad (3)$$

where  $T_i$ ,  $S_i$  are temperature and salinity of box  $i$ , and  $k$  is a constant linking volume transport  $m$  to density difference. For simplicity the equation of state has been linearized; its non-linearity is not relevant to the argument presented here.

The volume transport is determined by combining Eqs. 1 and 3, resulting in a quadratic equation

$$m^2 + k\alpha(T_2 - T_1)m + k\beta S_0 F_1 = 0 \quad (4)$$

yielding  $m$  as function of thermal and freshwater forcing:

$$m = -\frac{1}{2}k\alpha(T_2 - T_1) \pm \sqrt{\frac{1}{4}[k\alpha(T_2 - T_1)]^2 - k\beta S_0 F_1} \quad (5)$$

As in Stommel's original model, only solutions with the positive root are stable equilibria.

It is instructive to consider the roles of the atmospheric vapour transports  $F_1$  and  $F_2$ .  $F_1$  represents the vapour transport into the “catchment area” of NADW (which for the flow direction indicated consists of the combined surface areas of boxes 2 and 3), while  $F_2$  represents a vapour transport within the Atlantic catchment from low to high latitudes. Equation 5 shows that the equilibrium NADW flow depends only on the vapour transport  $F_1$  into the Atlantic catchment, not on the distribution within that catchment. This is an idealization of the box model, arising from the fact that all the freshwater added to box 3 will be transported into box 2 by the oceanic flow. In reality, part of the freshwater added to (or removed from) the tropical Atlantic would be transported south by the wind-driven flow, not affecting salinity in the northern high-latitudes. Freshwater added to the northern high-latitudes would therefore be more effective in influencing the NADW formation rate than freshwater added further south; this can be seen in the GCM experiments discussed later. The effect of the wind-driven flow could be simulated in the box model by adding diffusion between the boxes. The ‘active’ portion of the freshwater flux (i.e. that part which forces NADW flow and appears in Eq. 5) would then be  $F_1$  minus the diffusive flux. For the sake of simplicity, we do not consider the diffusive flux explicitly in the box model, we simply define  $F_1$  as the ‘active’ flux only. Note that this ‘active’ flux, which determines NADW formation rate, may have the opposite sign of the total surface flux into the ocean basin if the wind-driven freshwater transport more than cancels the surface flux; this is indeed the case in the GCM experiments.

The vapour flux from the low to the high latitudes of the Atlantic (here called  $F_2$ ), which is the control parameter of Stommel's (1961) hemispheric box model, plays only a minor role in the cross-equatorial flow. In equilibrium,  $F_2$  merely determines the meridional gradient ( $S_3 - S_2$ ). An increase in  $F_2$  makes the tropical ocean more saline and, since the mean salinity of the

box system must remain constant, reduces salinity everywhere else by an equal amount, considering that the gradient ( $S_2 - S_1$ ) is independent of  $F_2$ . Atmospheric transport within the basin (as modelled by  $F_2$ ) will lead to a latitude dependent oceanic freshwater transport. It is thus possible that the issue of whether the freshwater transport of the thermohaline flow is northward or southward could depend on latitude, though the GCM experiments suggest that this is not the case. In any case, it is the freshwater transport at the southern end of the basin (at  $30^\circ\text{S}$ ) which is relevant for the stability of the circulation; it shows whether the thermohaline flow has received a net freshwater input or loss along its route through the Atlantic. The freshwater transport at  $30^\circ\text{S}$  balances the active flux  $F_1$ , which in turn controls the NADW flow rate.

In addition to making the oceanic equilibrium freshwater transport latitude-dependent, the flux  $F_2$  affects the transient model response. A rapid increase of  $F_2$  dilutes the water in box 2, leading to a temporary reduction in NADW volume transport. With an advective time scale of centuries the model responds by adjusting the salinities in the boxes until the original volume transport is restored; the equilibrium transport being independent of  $F_2$ . In extreme cases (e.g. a massive meltwater influx), however, a transition to a new equilibrium with inverse flow may be triggered.

Having discussed the role of the freshwater forcing, we can now classify deep water flow (with  $m > 0$ ) in three dynamical regimes (see Fig. 2). If  $T_2 < T_1$  and  $F_1 < 0$ , salt and temperature gradients work together to drive the flow. Purely haline driven flow occurs for  $T_2 > T_1$  and  $F_1 < 0$ ; Eq. 5 shows that in this case the flow is zero for  $F_1 = 0$  and increases monotonically for increasing freshwater loss. Note that here haline driven flow has a different physical interpretation from in Stommel's hemispheric box model: it is not a flow with deep water formation in the tropics, but simply a flow driven by a salinity gradient between the northern high-latitude sinking region and the Atlantic outflow at  $30^\circ\text{S}$ . The most interesting regime is the purely thermally driven flow with  $T_2 < T_1$  and  $F_1 > 0$ , where freshwater forcing *brakes* the overturning. This solution

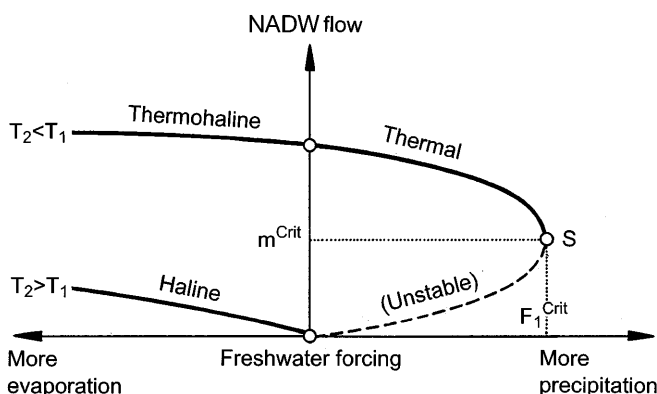


**Fig. 2.** The three flow regimes (solid) of the box model. The dashed line is an unconditionally unstable solution. *S* is the saddle-node bifurcation point

branch ends in a saddle-node bifurcation (point *S* in Figs. 2 and 7) at a critical freshwater input of  $F_1^{crit} = k\alpha^2(T_2 - T_1)^2 / 4\beta S_0$  and a volume transport of  $m^{crit} = k\alpha(T_1 - T_2) / 2$ . Note that the volume transport at the bifurcation is half the volume transport for zero freshwater forcing. This result holds exactly only for prescribed temperatures, but is still valid to a very good degree of accuracy if temperatures are allowed to vary in response to oceanic heat flux changes (see appendix). In contrast to the other two regimes, the overturning circulation now transports freshwater away from the NADW formation region. This is the situation found in the general circulation model experiments described later.

We have so far restricted the discussion to solutions with positive flow (i.e. the flow direction indicated on Fig. 1); the same solution structure exists, of course, also for reverse flow, but then  $F_2$  becomes the control parameter instead of  $F_1$ . This allows two equilibria with pole-to-pole flow in either direction for a completely symmetrical box model (i.e.  $T_1 = T_2$  and  $F_1 = -F_2$ ); such a symmetrical model with 3 boxes was presented by Rooth (1982). Both solutions are in this case purely haline driven; the pole-to-pole temperature gradient either vanishes (for fixed  $T_1 = T_2$ ) or inhibits the flow (if temperatures adjust in response to the oceanic heat transport towards the sinking region). The thermal flow branch, which is of prime interest for this study, is only possible for asymmetric forcing, i.e. it depends on the sinking region being *colder* than the region at  $30^\circ\text{S}$ . Our model thus differs conceptually from the model of Rooth; it explicitly considers the north-south asymmetry which arises from the enclosure of the Atlantic by continents north of  $30^\circ\text{S}$ . The arguments presented in this work suggest that this geographical north-south asymmetry is crucial for driving the Atlantic loop of the conveyor belt.

### 3 Global circulation model experiments

To test the ideas arising from the conceptual model, a series of experiments with a global ocean circulation model (Pacanowski et al. 1991) coupled to a simple energy balance atmosphere was performed. The model has a realistic topography with  $3.75^\circ \times 4.5^\circ$  resolution and 12 vertical levels; configuration and spinup procedure have been described in detail elsewhere (Rahmstorf 1995b). The experiments started from a steady equilibrium state corresponding to the present-day circulation, driven by observed winds (Hellerman and Rosenstein 1983) and a prescribed freshwater flux field derived from a spinup integration (Rahmstorf 1995b). A simple, radiative-diffusive atmospheric energy balance was used to allow for the feedback effect of oceanic heat transport on surface temperature (Rahmstorf and Willebrand 1995). The stream function for this equilibrium state is shown in Fig. 3, and the meridional overturning in the Atlantic in Fig. 9.

Freshwater flux perturbations were added to the ocean in different regions (see Fig. 4); starting from

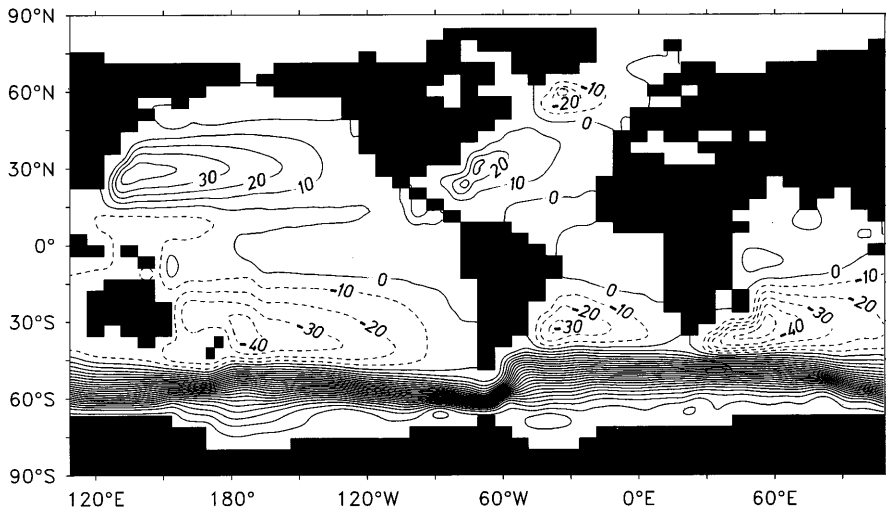


**Fig. 3.** Transport stream function of the global circulation model, contoured in Sv. Note the subtropical gyre of 35 Sv in the South Atlantic



**Fig. 4.** A map of the four different regions where freshwater forcing was perturbed by adding a slowly increasing flux. Global mean salinity was conserved by an opposite perturbation in the equatorial Pacific

zero, they were increased very slowly (at a rate of 0.05 Sv per 1000 years) to track the quasi-equilibrium response, as discussed by Rahmstorf (1995a). If the freshwater input is then decreased again at the same rate, the model goes through a characteristic hysteresis behaviour (see Rahmstorf 1995a for a detailed discussion). The hysteresis response for a perturbation in region B (marked on Fig. 4) is shown in Fig. 5. The figure shows that the NADW overturning rate declines when the freshwater input into region B is increased (the overturning rate is defined as the maximum of the meridional stream function shown in Fig. 9; the outflow of NADW at 30°S varies in step with the overturning rate in the experiments). There is a parameter region where solutions with two somewhat different rates of NADW formation exist for the same forcing: for the stronger overturning rate convection in the Labrador Sea is present, for the weaker rate it is absent. There is also a parameter region where stable states with and without NADW formation can exist for the same forcing. It is interesting that a freshening of the tropical Atlantic

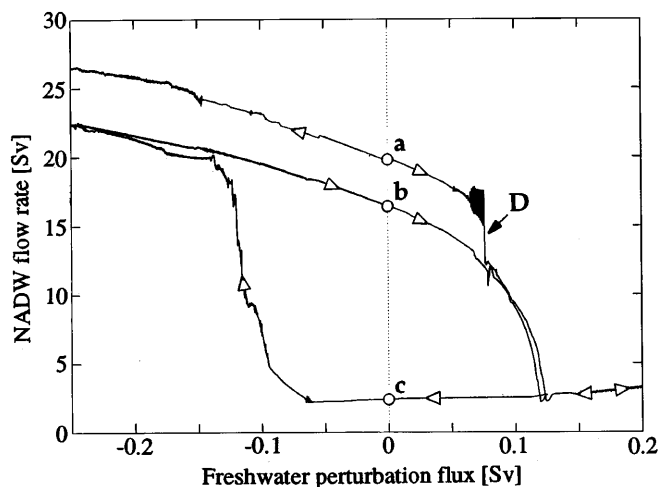


**Fig. 5.** Hysteresis response of the North Atlantic overturning to a slowly changing freshwater forcing (at a rate of 0.05 Sv/1000 y) in region B. Point a is the initial equilibrium state; from there the freshwater forcing was gradually increased until the right edge of the figure was reached, then decreased again moving through point c towards the left edge, then increased once more through point b. Open circles mark true equilibria as confirmed by continuing the integration with constant freshwater forcing for several thousand years. Point b is thus the final equilibrium reached after one (clockwise) hysteresis loop; it differs from a by the absence of Labrador Sea convection. Point c is a state with no NADW formation and all deep water forming in the Southern Hemisphere

leads to a decrease of NADW formation. In Stommel's hemispheric box model, and in box models which force separate Northern and Southern Hemisphere overturning cells (Thual and McWilliams 1992), the effect of tropical freshening would be to enhance the northern overturning, since it increases the equator-to-pole density gradient. Tropical freshening in these models has the opposite effect on NADW formation from high-latitude freshening, while in the box model shown in Fig. 1 it has the same effect as high-latitude freshening.

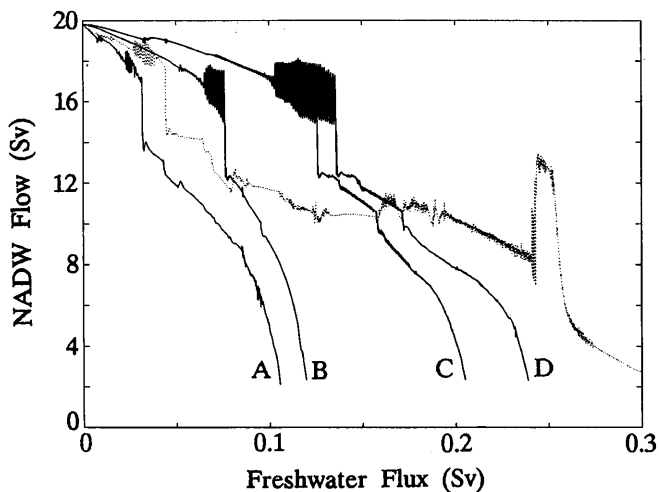


**Fig. 6.** Response of the NADW circulation to a slow increase in freshwater flux; the curves are labelled according to the region where the flux was added, as shown in Fig. 4. The  $x$ -axis shows the freshwater perturbation relative to the model equilibrium corresponding to present-day flow. The *dotted* curve shows the response to a flux perturbation in region *A* together with an opposite perturbation in region *B*; the *peak* near 0.25 Sv is due to convection at 42°N, 66°W. (This figure corresponds to the right half of Fig. 5; the curve labelled *B* is also found there.)

The effect of freshwater perturbations in different regions on the overturning rate of NADW is compared in Fig. 6. The gradual decline of the circulation with increased freshwater input corresponds closely to the box model behaviour for thermally driven flow (see later). The step-like discontinuity in the curves results from physics not included in the box model, namely the shutdown of convection in the Labrador Sea as analyzed in Rahmstorf (1995a). The further north the freshwater is added, the more effective it is in suppressing NADW flow. This is consistent with the idea that only a certain fraction of the freshwater added further south is 'active' in influencing NADW formation. Based on the assumption that 100% of the freshwater added to region *A* is 'active', we can estimate the 'active' portions in other regions (Table 1); these must be interpreted with caution, however, since they cannot be assumed to be constant and may depend on the flow.

The dotted line in Fig. 6 shows an experiment where freshwater was moved from region *B* to region *A*, corresponding to a change in  $F_2$  in the conceptual model (plus a small change in  $F_1$  due to the smaller 'active' portion in region *B*). Judged by the small slope of the smooth sections of the curve, the equilibrium NADW flow is indeed not very sensitive to such a forcing change, at least not through the advective mechanism

**Table 1.** Percentage of the freshwater added to a given region which is 'active' in affecting NADW formation

Region	A	B	C	D
Active freshwater %	100	88	51	44

captured by the box model. Flow changes are dominated instead by rearrangements of convection (Rahmstorf 1995a): first the shut down of Labrador convection, then the start up of convection further south, and finally the shut down of this new convection site and the subsequent collapse of the circulation.

To demonstrate the close correspondence between the global circulation model and the box model, their hysteresis response to an identical freshwater forcing cycle was determined (Fig. 7): freshwater forcing was increased linearly at the above rate and then decreased again to its initial value. For the comparison, we used the lower of the two hysteresis loops shown in Fig. 5, i.e. the global model was started from a state with no Labrador convection (to avoid the discontinuity when it shuts down) but with a freshwater forcing of  $-0.25$  Sv relative to the present-day forcing field. In the box model, the flow constant  $k$  and the driving temperature gradient ( $T_2 - T_1$ ) were tuned to match the global model result. The absolute magnitude of the flow is set by  $k$ , while the dimensionless ratio of freshwater forcing and flow at the bifurcation, i.e. the ratio of 'width' to 'height' of the hysteresis loop, depends only on  $(T_2 - T_1)$ . To obtain the match shown  $k = 6.0 \text{ y}^{-1}$ , and the driving temperature difference was 5.9°C. This is again consistent with the idea that it is not the equator-to-pole temperature difference which is responsible for driving the flow, as in Stommel's model, but the smaller difference between formation and outflow region of NADW.

A slight complication arises because the magnitude of the 'active' freshwater forcing ( $F_1$  for the box model) is not known for the GCM. Therefore, the zero point of the freshwater axis is that of the box model,

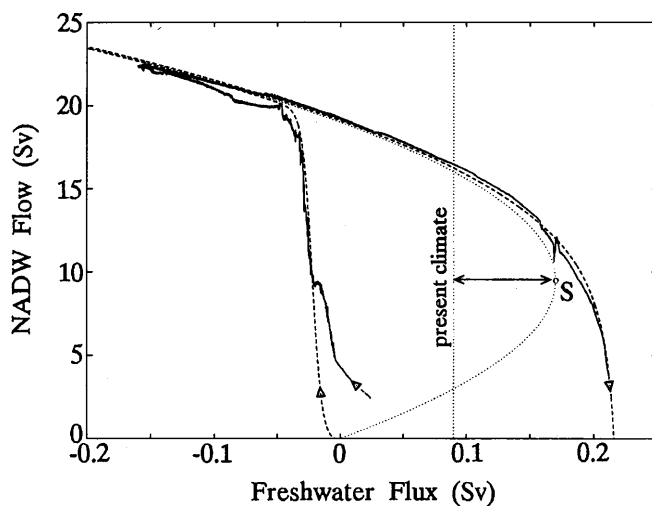


**Fig. 7.** Hysteresis curves of box model (*dashed*) and global circulation model (*solid*). Also shown is the equilibrium curve of the box model (*dotted*) with the saddle-node bifurcation point *S*. The equilibrium branch below *S* is unconditionally unstable. The zero point of the freshwater axis is that of the box model, since the corresponding point is not known in the circulation model; the *vertical dotted line* at 0.09 Sv marks the 'present-day' freshwater flux of the latter. The *arrow* marks the distance of the present climate from the bifurcation

and the origin of the GCM freshwater flux was chosen so that the hysteresis curves match. The initial state of the GCM with 'present-day' forcing is then located on the dotted line, suggesting that the conveyor belt in this model state receives a net freshwater input of 0.09 Sv during its passage through the Atlantic. (Strictly speaking, the freshwater flux values for the global model would need to be rescaled slightly, to account for the fact that they are given in terms of the total flux perturbation rather than 'active' flux, but since we estimated the difference to be only 12% for region *B* this was not done here.) The box model fit further suggests that the 'present day' state is 0.07 Sv away from the bifurcation point *S*, beyond which NADW formation cannot be sustained. A similar value (0.06 Sv) was found in direct experiments with the global model (Rahmstorf 1995a). The present-day circulation in the global model is thus on a thermally driven branch and close to a bifurcation, with freshwater forcing inhibiting the flow. This requires that the NADW circulation must transport freshwater *southward*, in spite of the freshwater export from the Atlantic basin by the atmosphere. To understand this, we will take a closer look at the freshwater budget of the circulation in the next section.

The excellent agreement of box model and global model suggests that the dynamics governing NADW flow in the circulation model must be surprisingly simple; the box model simply assumes that the flow is proportional to the density difference  $\Delta\rho$  (Eq. 3), following Stommel's (1961) original ad-hoc assumption. Other authors have argued that the flow should be proportional to  $(\Delta\rho)^2$  (Cessi and Young 1992; Cessi 1994), while scaling arguments suggest that the power law should be  $(\Delta\rho)^{1/3}$  (Welander 1986; Bryan 1987; Rahmstorf 1995c). Figure 8 shows the relationship for the global model: it is linear over the whole flow range from 2 Sv to 22 Sv. A linear flow law was previously found in an idealized basin model by Hughes and Weaver (1994).

The classical scaling argument uses the thermal wind equation to obtain a velocity scale depending on the density structure:

$$u = \frac{g}{2\Omega} \frac{D}{L} \Delta\rho \quad (6)$$

where  $\Omega$  is the angular frequency of the Earth,  $L$  is a horizontal length scale and  $D$  is the scale depth over which density changes in the vertical. This thermocline depth  $D$  depends on the vertical upwelling-diffusion balance, leading to the power law of  $(\Delta\rho)^{1/3}$ . However, if  $D$  were independent of the NADW flow rate, we would obtain a linear flow law. This would be consistent with the assumption that NADW does not upwell within the Atlantic basin and thus does not influence  $D$  in the way assumed in the classical scaling argument. As discussed earlier, our box model (Fig. 1) also reflects this assumption of no upwelling across the tropical thermocline. The scaling argument directly only explains a *zonal* flow, but because it is constrained by

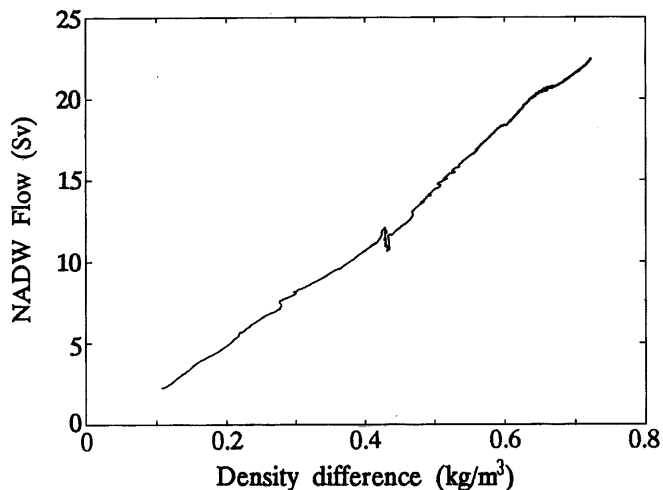


**Fig. 8.** Dependence of NADW flow on the density difference between two boxes in the NADW formation and outflow regions in the global circulation model. The figure shows the difference in average densities of two latitudinal strips (the former from 50–55°N, the latter from 35–40°S) at mid-depth (750 m). Similar linear relations hold also at other depths and for depth averages, as well as for different averaging regions, though slope and offset from the origin obviously depend on the region chosen

continental boundaries, a secondary meridional flow arises (see Wright et al. 1995).

#### 4 Freshwater budget of the conveyor

The reason why the direction of the freshwater transport of the NADW circulation is not clear a priori is that salinity does not decrease monotonically with depth, as temperature does, but has a minimum in the intermediate water at about 1 km depth. The freshwater budget of the conveyor belt therefore depends on the relative contributions of low salinity intermediate water and high salinity thermocline water to the northward limb of the conveyor. North of the northern limit of intermediate water at circa 20°N, the NADW overturning freshwater transport can only be southward.

The situation is illustrated in Figs. 9 and 10, which show the salinity distribution in the global model north-south and in a section at 30°S. Superimposed is the flow. The tongue of intermediate water is clearly visible at ca. 800 m depth, though somewhat less pronounced in the 12-level model than in the observed 33-level climatology (Levitus et al. 1994): at 33°S, the salinity minimum in the intermediate water is 34.46 psu in the model (34.29 psu in the climatology), the maximum in the core of NADW is 34.84 psu (34.93 psu). The upper ocean flow across 33°S is dominated by the horizontal gyre circulation with southward flow at the western boundary and northward flow in the eastern basin (see also Fig. 3). Combined with the strong zonal salinity gradient near the surface, this leads to a large freshwater import. The southward flow of NADW and northward flow of Antarctic Bottom Water are also visible.

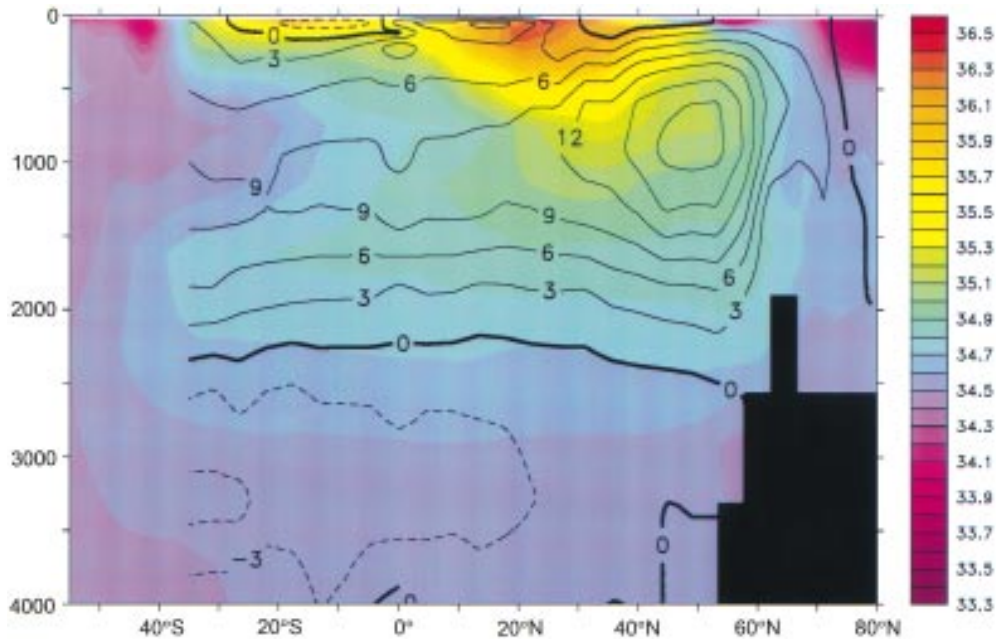


**Fig. 9.** Atlantic overturning stream function (contoured in Sv) for the 'present-day' equilibrium of the global model, superimposed on a plot of Atlantic zonal-mean salinity

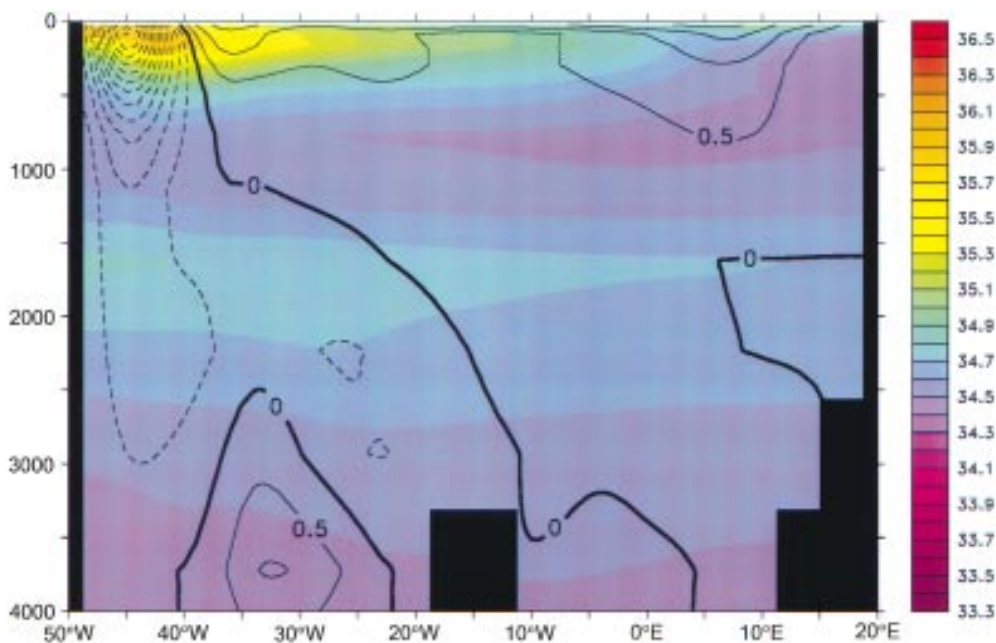


**Fig. 10.** Zonal section of meridional flow (contoured in cm/s) and salinity (colour) at 30°S in the global model

The resulting freshwater transport of the model is shown in Fig. 11. For comparison, the freshwater transport from the inverse model of Schiller (1995) and that implied by the freshwater climatology of Baumgartner and Reichel (1975) are also shown. The latter curve is obtained by integrating surface fluxes and river runoff southward from the arctic, and therefore has an error that accumulates towards the south; at 35°S it was estimated as 0.6 Sv (Wijffels et al. 1992). Following Schmitt et al. (1989), 2/3 of Amazon water was added north of the equator and 1/3 south of the equator in the integration. Schiller's inverse model of the Atlantic, in contrast, is tied to the observed salinity and temperature distribution at 30°S (Schiller restores temper-

ature and salinity to the climatology of Levitus 1982 at time scales of 30–250 days, depending on depth, south of 30°S). It uses the adjoint method to find an optimal model solution north of this latitude, which best agrees with the observed surface fluxes, salinities and temperatures. Arguably, this method should lead to more reliable freshwater transport estimates than simple integration of surface fluxes; dynamics and observed ocean salinities are used to constrain the budget, thus avoiding an accumulating integration error.

The freshwater transport of the global model used here and of Schiller's (1995) inverse model of the Atlantic agree well. They deviate from the Baumgartner and Reichel (1975) data, although they remain within

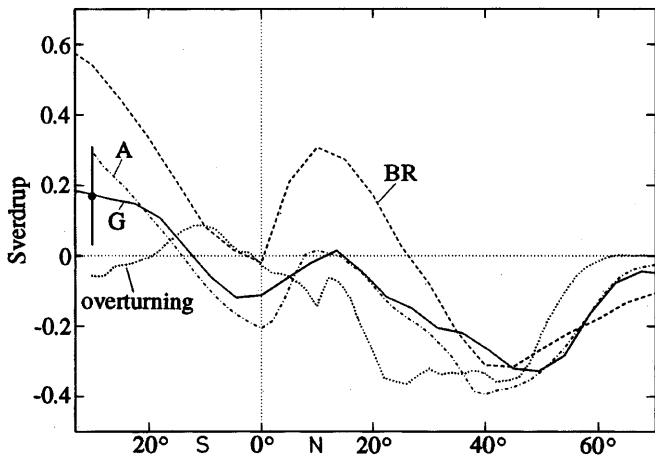


**Fig. 11.** Meridional freshwater transport in the Atlantic in the global model (*solid*), in Schiller's (1995) Atlantic model (*dash-dotted*) and from Baumgartner and Reichel's (1975) world water balance (*dashed*). The *dotted* line shows the *overturning component* (Eq. 6) of Schiller's model. The data point at 30°S was calculated in a way consistent with the definition of freshwater transport used here, using a recent hydrographic section of RV Meteor (Holfort 1994). A Russian estimate (Dobrolyubov 1991) gives  $0.29 \pm 0.09$  Sv at 32°S

the large error margin of the latter. All three agree that the Atlantic basin north of 30°S is a net evaporative basin, losing freshwater at a rate of 0.2–0.55 Sv. This freshwater loss must be balanced in equilibrium by a net freshwater inflow from the ocean circulation.

The balancing transport can be achieved either by the vertical overturning associated with the conveyor belt, or by the wind-driven circulation (Schiller concludes that diffusive transports play only a minor role). While there is no rigorous way of separating these components, a useful working definition of the overturning component of freshwater transport is

$$F_{OT} = -\frac{1}{S_0} \int \bar{v} \bar{S} dz \quad (7)$$

where  $\bar{S}$  and  $\bar{v}$  are the zonally averaged salinity and integrated northward velocity (note that the net volume transport across the section,  $\int \bar{v} dz$ , vanishes, since the Atlantic is closed in the north in this model). This quantity  $F_{OT}$  is included in Fig. 11; it is negative, i.e. the overturning freshwater transport is southward at all latitudes except just south of the equator, where an Ekman cell is responsible for some northward transport. The wind-driven gyre transport is thus the largest term in the freshwater budget and balances not only the net freshwater loss from the Atlantic basin through the atmosphere, but also an additional freshwater export by the conveyor belt. This freshwater budget is plausible, because the surface freshwater loss of the Atlantic arises in the subtropical gyre of the South Atlantic, the North Atlantic has zero freshwater loss or may even gain freshwater (see Fig. 11). The freshwater budget is also consistent with Fig. 7, which suggests that the present NADW circulation in the model receives net precipitation.

Further illustration of this freshwater budget can be obtained by comparing model salinities for circulation states with and without NADW circulation, with the same prescribed freshwater fluxes. The salinity difference between model states *a* and *c* (marked on Fig. 5) is shown in Figs. 12 and 13. The figures show that the entire Atlantic gets fresher when the conveyor belt is 'off', consistent with the idea that the conveyor belt acts to export freshwater from the Atlantic. As the global salt content is constant, the other oceans get saltier. Figure 12a is very similar to the corresponding figure for the coupled model of Manabe and Stouffer (1988), suggesting that the direct effect of the oceanic salt transport dominates any changes in the atmospheric freshwater transport occurring in the coupled model. In our GCM there is thus no salt accumulation in the Atlantic during times of weak NADW flow as required for the simple 'salt oscillator' mechanism originally proposed by Broecker et al. (1990a). Such an oscillator could only work if other feedbacks lead to salt accumu-

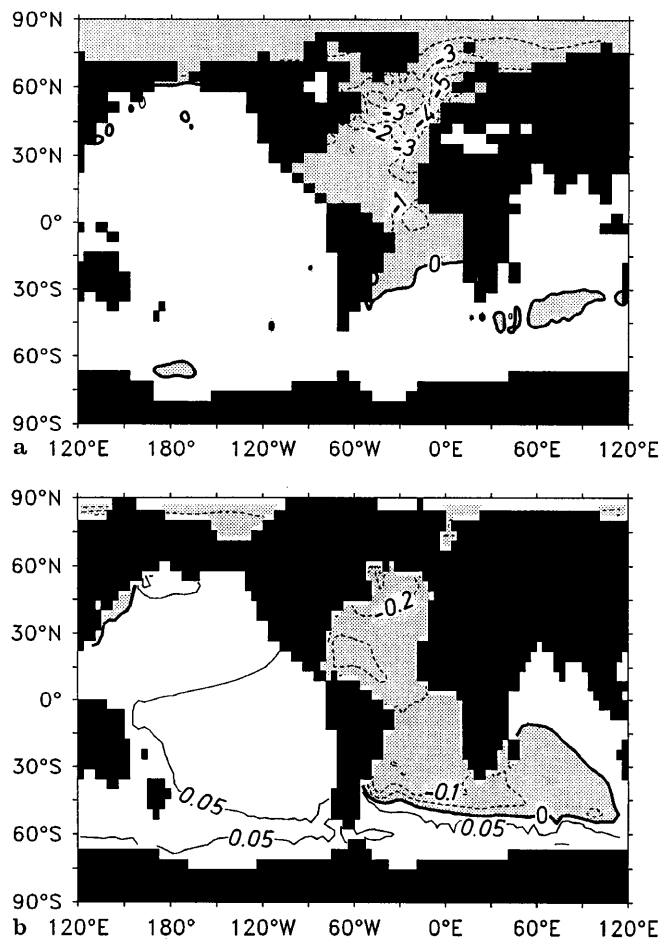


**Fig. 12a, b.** Salinity of states *c* minus *a* of the GCM (see Fig. 5), for the surface (*top*) and at 2 km depth. In the absence of NADW formation, the Atlantic gets fresher and the other oceans saltier. Note the fresher tongue extending out of the Atlantic in 2 km depth; this is the region directly affected by salty NADW outflow in the 'present day' equilibrium *a*

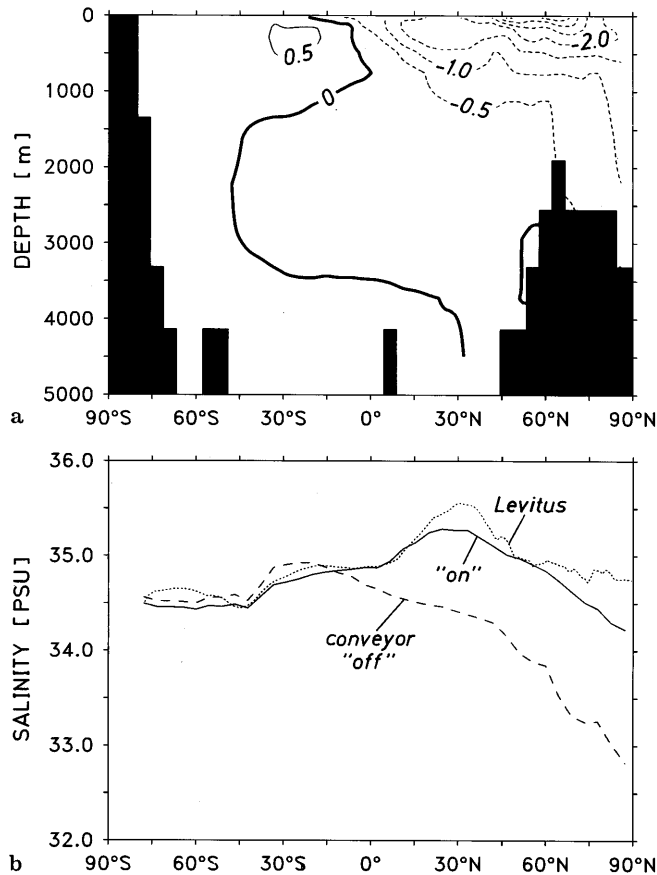


**Fig. 13a, b.** The salinity difference between states *a* and *c* in the Atlantic shown as zonal average (*top*), and the zonal mean salinities averaged again over the top 2 km (*bottom*). Also included is the same quantity computed from the data of Levitus et al. 1994. In the absence of NADW formation, Atlantic salinity decreases north of 20°S and increases south of this latitude, consistent with a southward freshwater transport due the NADW circulation

lation, e.g. reduced run-off from continental ice sheets during periods of weak NADW flow (Birchfield et al. 1993).

It is often stated that the saline outflow of NADW from the Atlantic enhances the salinity of Circumpolar Deep Water (CDW) and even the deep waters of the Pacific and Indian Oceans. This is true if we consider the NADW outflow in isolation, rather than as a circulation system together with its upper, northward flow. If we look at the combined effect as in Figs. 12 and 13, we notice that although NADW is the most saline deep water source for the present circulation, most of the world ocean would get saltier in the absence of NADW formation, the exception being the Atlantic and a tongue emanating eastward from it. This is because in the GCM, the high salinity of NADW is not created by surface forcing in the Atlantic, but is derived from outside the Atlantic; the conveyor belt enters the Atlantic at 30°S in the Benguela Current at a higher salinity than that of NADW. Gordon et al. (1992) have proposed that this inflow is salt-enriched as a result of evaporation in the Indian Ocean. In the absence of NADW formation, these saline waters

would find a more direct route into the deep water, instead of travelling through the Atlantic getting diluted along the way.

Stommel (1980) has tried to balance the mass, heat and salt budgets north of 30°S by a vertical overturning motion with three water masses (mid-thermocline, intermediate and deep water) of given temperatures and salinities. Balancing the Atlantic in this way required an overturning of 92 Sv; a refined version of this model (Piola and Gordon 1986) still required a value of 54 Sv NADW outflow at 30°S, rather than the observed ca. 12 Sv. The reason why these budget calculations fail is their neglect of the heat and freshwater transport of the wind-driven subtropical gyre in the South Atlantic, which we have shown to be the largest term in the freshwater budget, balancing the net evaporation of the Atlantic basin and the conveyor's freshwater export in the global GCM. Repeating the budget calculation with the same water masses as Piola and Gordon (1986), but balancing only the overturning transport components found in Schiller's (1995) inverse model (0.36 PW northward heat transport, 0.06 Sv southward freshwater transport) leads to a more realistic NADW outflow of 10.9 Sv, compensated by a northward flow of 8.2 Sv mid-thermocline water and 2.7 Sv intermediate water.

## 5 Discussion

The response of the GCM to freshwater perturbations at different latitudes shows that the NADW circulation behaves as a continuous conveyor belt flow driven by a density gradient between the North and the South Atlantic, rather than as a superposition of more locally driven, hemispheric overturning cells. The conceptual model presented in Fig. 1 takes this into account and reproduces the behaviour of the GCM remarkably well (Fig. 7). It shows that there are three dynamical regimes for the Atlantic conveyor belt: it is either thermally driven, haline driven or both. Since the GCM response to freshwater anomalies shows a saddle-node bifurcation at a critical freshwater perturbation of 0.06 Sv and a critical NADW transport of 12 Sv (Rahmstorf 1995a), the GCM circulation must be thermally driven (i.e. on the upper solution branch in Fig. 2); the purely haline branch does not have this bifurcation. The thermal driving is due to the upper ocean temperatures being colder in the deep water formation regions than at the outflow latitude of 30°S. The enclosure of the Atlantic by continents between 30°S and high northern latitudes, and the associated geographical north-south asymmetry are thus crucial to the concept.

The direction of the freshwater transport associated with the conveyor belt depends on where on the solution branch the present day circulation is located. If the circulation is in the left half of Fig. 2, it is thermally and haline driven, i.e. undergoes a salinity increase during its passage through the Atlantic and transports freshwater northward. If it is in the right half of Fig. 2, the

circulation transports freshwater southward. In this case, the freshwater forcing opposes the thermal driving, and equilibria with and without NADW formation exist.

The present-day equilibrium state of the GCM, derived using observed surface temperatures, salinities and winds, is located on the purely thermal branch, in a flow regime inhibited by net freshwater input and not far from Stommel's bifurcation point (Fig. 7). It therefore transports freshwater southward out of the Atlantic, in spite of the Atlantic being a net evaporative basin. The freshwater loss of the Atlantic due to evaporation and the conveyor belt flow is balanced by a large freshwater import in the wind-driven subtropical gyre in the South Atlantic. In other words, the dynamic regime and stability of the Atlantic conveyor belt is the result of a complex salinity balance depending on atmospheric fluxes, the freshwater import by the subtropical gyre and the transport by the conveyor belt itself. It is by no means certain that a coarse-resolution GCM reproduces this balance correctly. A GCM with a very weak South Atlantic subtropical gyre (e.g. Maier-Reimer et al. 1993), or a two-dimensional model with no horizontal circulation (e.g. Stocker and Wright 1991), may reside on a rather different position in the stability diagram. To understand the stability of the thermohaline circulation in a particular model, a diagnosis of its freshwater balance is required.

The southward freshwater transport of the conveyor in our GCM is due to its northward flow across 30°S occurring predominantly in the saline surface water. It is encouraging that this freshwater balance is supported by results from Schiller's (1995) inverse model. However, it is at variance with the inverse calculation of Schlitzer (1996), which requires the northward flow to be predominantly in the fresher intermediate water, in order to reproduce the observed low-salinity tongue. The relative contribution of surface and intermediate water to the northward inflow is thus still an open question; this issue is closely linked to the debate over the relative importance of the 'cold water route' and the 'warm water route' for the conveyor belt (Gordon 1986; Rintoul 1991).

While the simple conceptual model of NADW flow presented here explains much of the behaviour of the global circulation model, the theory is not complete. It does not deal with the transient response of the circulation during rapid climate changes, it captures only the large-scale *advective* feedback, not the effect of *convection* changes (Rahmstorf 1994), and it applies only north of about 30°S, where the flow is confined between continents. Different dynamics determine how the deepwater loop is closed south of this latitude, where NADW joins the Antarctic Circumpolar Current.

The picture that emerges from this and previous modelling studies (see the review of Rahmstorf et al. 1996) is of an Atlantic thermohaline circulation in a precarious dynamical balance close to Stommel's bifurcation point, with thermal and freshwater forcing pulling in opposite directions. The stability of this circula-

tion in a changing climate is therefore a serious concern; a weakening of thermal forcing or an increase in 'active' freshwater input could push the circulation beyond the bifurcation. To confirm whether the models locate the thermohaline circulation in the correct place on the stability diagram, observational studies need to establish the exact freshwater balance at 30°S in the Atlantic. The challenge here is to decompose the freshwater transport into wind-driven and 'conveyor belt' components.

## Appendix

The conceptual model (Eqs. 1–5) was considered for prescribed temperatures of the boxes. In reality, temperatures adjust to changes in oceanic heat transport, leading to a feedback effect on the circulation (Rahmstorf and Willebrand 1995). To take this into account, we can couple the box temperatures to prescribed values through a Newtonian restoring law; the limit of very strong coupling (short restoring time scale) is then the case of prescribed temperatures. In addition to the equilibrium conditions Eqs. (1–3), we get three thermal balances:

$$m(T_2 - T_1) = \gamma(T_1 - T_1^*) \quad (8)$$

$$m(T_1 - T_3) = \gamma(T_3 - T_3^*) \quad (9)$$

$$m(T_3 - T_2) = \gamma(T_2 - T_2^*) \quad (10)$$

where  $T_i^*$  are the restoring temperatures and  $\gamma$  is the thermal coupling constant. These can be combined to

$$T_2 - T_1 = T_2^* - T_1^* + \frac{\gamma m [T_1^* + T_3^* - 2T_2^*] - 3m^2(T_2^* - T_1^*)}{\gamma^2 + 3\gamma m + 3m^2} \quad (11)$$

Assuming that the surface coupling is stronger than the effect of oceanic heat transport,  $m/\gamma \ll 1$  and we can consider only the leading order in  $m/\gamma$ ; this will show the leading order of the temperature feedback effect. Equation 11 simplifies to

$$T_2 - T_1 \approx T_2^* - T_1^* + \frac{m}{\gamma} [T_1^* + T_3^* - 2T_2^*] \quad (12)$$

Inserting this in Eq. 4 gives the modified equilibrium flow condition as

$$\left[ 1 + \frac{k\alpha}{\gamma} (T_1^* + T_3^* - 2T_2^*) \right] m^2 + k\alpha (T_2^* - T_1^*) m + k\beta S_0 F_1 = 0 \quad (13)$$

This is again a quadratic equation for  $m$ , so that the shape of the solution curve is the same as for prescribed temperatures (Fig. 2), and we would have obtained an equally good fit in Fig. 7 with this modified model. In particular, the volume transport at the bifurcation (obtained from the condition  $dF_1/dm = 0$ ) is

$$m^{crit} = \frac{1}{2} \frac{k\alpha (T_1^* - T_2^*)}{1 + \frac{k\alpha}{\gamma} (T_1^* + T_3^* - 2T_2^*)} \quad (14)$$

which is still  $m^{crit} = m_0/2$ , i.e. half the flow for zero freshwater forcing; deviations from this only arise in the second order in  $m/\gamma$ .

The main effect of the temperature response is thus to provide a negative feedback on the flow, since the temperature difference ( $T_1 - T_2$ ), which drives the flow, is reduced for increasing oceanic heat transport; to first order this rescales the solution curve without changing its shape.

*Acknowledgements.* Stimulating discussions with Wally Broecker, Jochem Marotzke and Jürgen Willebrand helped to clarify the ideas presented in this work and are gratefully acknowledged. I am indebted to Matthew England for sharing his model code, to Andreas Schiller for providing data from his inverse model, and to Steve Hankin for advice on the Ferret graphics package. Special thanks to Dulcie Smart for carefully editing the manuscript. The work was funded by the German Science Ministry (BMBF).

## References

- Baumgartner A, Reichel E (1975) The world water balance. Elsevier, Amsterdam
- Birchfield GE, Broecker WS (1990) A salt oscillator in the glacial North Atlantic? 2. A scale analysis model. *Paleoceanography* 5:835–843
- Birchfield GE, Wang H, Rich JJ (1994) Century/millennium internal climate variability: an ocean-atmosphere-continental ice sheet model. *J Geophys Res* 99:12459–12470
- Böning CW, Holland WR, Bryan FO, Danabasoglu G, McWilliams JC (1995) An overlooked problem in model simulations of the thermohaline circulation and heat transport in the Atlantic Ocean. *J Clim* 8:516–523
- Boyle EA, Keigwin L (1987) North Atlantic thermohaline circulation during the past 20000 years linked to high-latitude surface temperature. *Nature* 330:35–40
- Broecker WS (1991) The great ocean conveyor. *Oceanography* 4:79–89
- Broecker WS, Denton GH (1989) The role of ocean-atmosphere reorganisations in glacial cycles. *Geochim Cosmochim Acta* 53:2465–2501
- Broecker WS, Peteet DM, Rind D (1985) Does the ocean-atmosphere system have more than one stable mode of operation? *Nature* 315:21–26
- Broecker WS, Bond G, Klas M, Bonani G, Wolfi W (1990a) A salt oscillator in the glacial North Atlantic? 1. The concept. *Paleoceanography* 5:469–477
- Broecker WS, Peng TH, Jouzel J, Russell G (1990b) The magnitude of global fresh-water transports of importance to ocean circulation. *Clim Dyn* 4:73–79
- Bryan F (1986) High-latitude salinity and interhemispheric thermohaline circulation. *Nature* 323:301–304
- Bryan F (1987) Parameter sensitivity of primitive equation ocean general circulation models. *J Phys Oceanogr* 17:970–985
- Cessi P (1994) A simple box model of stochastically forced thermohaline flow. *J Phys Oceanogr* 24:1911–1920
- Cessi P, Young WR (1992) Multiple equilibria in two-dimensional thermohaline circulation. *J Fluid Mech* 241:291–309
- Dobrolyubov SA (1991) Estimate of the freshwater component of meridional water transport in the ocean. *Meteorol Gidrol* 1:71–78
- Gordon AL (1986) Inter-ocean exchange of thermocline water. *J Geophys Res* 91:5037–5046
- Gordon AL, Weiss RF, Smethie WM, Warner MJ (1992) Thermocline and intermediate water communication between the South Atlantic and Indian Oceans. *J Geophys Res* 97:7223–7240
- Hellerman S, Rosenstein M (1983) Normal monthly wind stress over the world ocean with error estimates. *J Phys Oceanogr* 13:1093–1104
- Holfort J (1994) Grossräumige Zirkulation und meridionale Transporte im Südatlantik. PhD Dissertation, Institut für Meereskunde, Kiel, Germany
- Hughes TMC, Weaver AJ (1994) Multiple equilibria of an asymmetric two-basin ocean model. *J Phys Oceanogr* 24:619–637
- Keigwin LD, Curry WB, Lehman SJ, Johnsen S (1994) The role of the deep ocean in North Atlantic climate change between 70 and 130 kyr ago. *Nature* 371:323–326
- Levitus S (1982): Climatological atlas of the world ocean, NOAA Professional Paper, vol 13. US Department of Commerce, NOAA, Washington DC
- Levitus S, Burgett R, Boyer T (1994) World ocean atlas 1994, vol 3: Salinity. US Government Printing Office, Washington, DC (NOAA Atlas NESDIS 3)
- Maier-Reimer E, Mikolajewicz U, Hasselmann K (1993) Mean circulation of the Hamburg LSG OGCM and its sensitivity to the thermohaline surface forcing. *J Phys Oceanogr* 23:731–757
- Manabe S, Stouffer RJ (1988) Two stable equilibria of a coupled ocean-atmosphere model. *J Clim* 1:841–866
- Marotzke J (1990) Instabilities and multiple equilibria of the thermohaline circulation. PhD Dissertation, Christian-Albrechts-Universität Kiel, Germany
- Marotzke J (1994) Ocean models in climate problems. In: Malanotte-Rizzoli P, Robinson AR (eds) Ocean processes in climate dynamics: global and Mediterranean examples. Kluwer, Dordrecht
- Pacanowski R, Dixon K, Rosati A (1991) The GFDL modular ocean model users guide, GFDL ocean group technical report edn, vol 2. GFDL, Princeton, USA
- Piola AR, Gordon AL (1986) On oceanic heat and freshwater fluxes at 30S. *J Phys Oceanogr* 16:2184–2190
- Rahmstorf S (1994) Rapid climate transitions in a coupled ocean-atmosphere model. *Nature* 372:82–85
- Rahmstorf S (1995a) Bifurcations of the Atlantic thermohaline circulation in response to changes in the hydrological cycle. *Nature* 378:145–149
- Rahmstorf S (1995b) Climate drift in an OGCM coupled to a simple, perfectly matched atmosphere. *Clim Dyn* 11:447–458
- Rahmstorf S (1995c) Multiple convection patterns and thermohaline flow in an idealised OGCM. *J Clim* 8:3028–3039
- Rahmstorf S, Marotzke J, Willebrand J (1996) Stability of the thermohaline circulation. In: Krauss W (ed) The warm water sphere of the North Atlantic Ocean. Bornträger, Stuttgart
- Rahmstorf S, Willebrand J (1995) The role of temperature feedback in stabilizing the thermohaline circulation. *J Phys Oceanogr* 25:787–805
- Reason CJC, Power SB (1994) The influence of Bering Strait on the circulation in a coarse resolution global ocean model. *Clim Dyn* 9:363–369
- Reid JL (1979) On the contribution of the Mediterranean Sea outflow to the Norwegian-Greenland Sea. *Deep-Sea Res* 26:1199–1223
- Rintoul SR (1991) South Atlantic interbasin exchange. *J Geophys Res* 96:2675–2692
- Roemmich DH, Wunsch C (1985) Two transatlantic sections: Meridional circulation and heat flux in the subtropical North Atlantic Ocean. *Deep-Sea Res* 32:619–664
- Rooth C (1982) Hydrology and ocean circulation. *Progr Oceanogr* 11:131–149
- Sarnthein M, Winn K, Jung SJA, Duplessy JC, Labeyrie L, Erlenkeuser H, Ganssen G (1994) Changes in east Atlantic deepwater circulation over the last 30000 years: Eight time slice reconstructions. *Paleoceanography* 9:209–267
- Schiller A (1995) The mean circulation of the Atlantic Ocean north of 30S determined with the adjoint method applied to an ocean general circulation model. *J Mar Res* 53:453–497

- Schlitzer R (1996) Mass and heat transports in the South Atlantic derived from historical hydrographic data. In: Wefer G, Berger WH, Siedler G, Webb D (eds) *The South Atlantic: present and past circulation*. Springer, Heidelberg Berlin New York
- Schmitt RW, Bogden PS, Dorman CE (1989) Evaporation minus precipitation and density fluxes for the North Atlantic. *J Phys Oceanogr* 19:1208–1221
- Stocker TF, Wright DG (1991) Rapid transitions of the ocean's deep circulation induced by changes in surface water fluxes. *Nature* 351:729–732
- Stommel H (1961) Thermohaline convection with two stable regimes of flow. *Tellus* 13:224–230
- Stommel H (1980) Asymmetry of interoceanic freshwater and heat fluxes. *Proc Natl Acad Sci USA* 77:2377–2381
- Thual O, McWilliams JC (1992) The catastrophe structure of thermohaline convection in a two-dimensional fluid model and a comparison with low-order box models. *Geophys Astrophys Fluid Dyn* 64:67–95
- Warren BA (1981) Deep circulation of the World Ocean. In: Warren BA, Wunsch C (eds) *Evolution of physical oceanography*. MIT Press, Cambridge, Ma., USA
- Warren BA (1983) Why is no deep water formed in the North Pacific? *J Mar Res* 41:327–347
- Weaver AJ, Hughes TMC (1992) Stability and variability of the thermohaline circulation and its link to climate. In: *Research Trends Series: trends in physical oceanography*. Council of Scientific Research Integration, Trivandrum, India
- Welander P (1986) Thermohaline effects in the ocean circulation and related simple models. In: Willebrand J, Anderson DLT (eds) *Large-scale transport processes in oceans and atmosphere*. Reidel, Dordrecht
- Weyl PK (1968) The role of the oceans in climate change: a theory of the ice ages. *Meteorol Mon* 8:37
- Wijffels SE, Schmitt RW, Bryden HL, Stigebrandt A (1992) Transport of freshwater by the oceans. *J Phys Oceanogr* 22:155–162
- Wright DG, Vreugdenhil CB, Hughes TMC (1995) Vorticity dynamics and zonally averaged ocean circulation models. *J Phys Oceanogr* 25:2141–2154
- Zaucker F, Broecker WS (1992) The influence of atmospheric moisture transport on the fresh water balance of the Atlantic drainage basin: general circulation model simulations and observations. *J Geophys Res* 97:2765–2773